Published in final edited form as:
Cell. 2013 September 26; 155(1): . doi:10.1016/j.cell.2013.09.003.

Mitofusin 2 in POMC Neurons Connects ER Stress with Leptin Resistance and Energy Imbalance

Marc Schneeberger[1,2,3], **Marcelo O Dietrich**[4,5], **David Sebastián**[3,6,7], **Mónica Imbernón**[8,9], **Carlos Castaño**[1,3], **Ainhoa Garcia**[1,3], **Yaiza Esteban**[1,3], **Alba Gonzalez-Franquesa**[1], **Ignacio Castrillón Rodríguez**[3,6,7], **Analía Bortolozzi**[10,11], **Pablo M Garcia-Roves**[1,3], **Ramon Gomis**[1,2,3], **Ruben Nogueiras**[8,9], **Tamas L Horvath**[4], **Antonio Zorzano**[3,6,7], and **Marc Claret**[1,3]

[1]Diabetes and Obesity Research Laboratory, Institut d'Investigacions Biomèdiques August Pi i Sunyer (IDIBAPS), 08036 Barcelona, Spain

[2]Department of Endocrinology and Nutrition, Hospital Clínic. School of Medicine, University of Barcelona, 08036 Barcelona, Spain

[3]CIBER de Diabetes y Enfermedades Metabólicas Asociadas (CIBERDEM), 08036 Barcelona, Spain

[4]Program in Integrative Cell Signaling and Neurobiology of Metabolism, Section of Comparative Medicine, Yale University School of Medicine, New Haven, CT 06520, USA

[5]Department of Biochemistry, Universidade Federal do Rio Grande do Sul, Porto Alegre RS 90035, Brazil

[6]Institute for Research in Biomedicine (IRB Barcelona), 08028 Barcelona, Spain

[7]Departament de Bioquímica i Biologia Molecular, Facultat de Biologia, Universitat de Barcelona, 08028 Barcelona, Spain

[8]Department of Physiology, School of Medicine, University of Santiago de Compostela–Instituto de Investigación Sanitaria, 15782 Santiago de Compostela, Spain

[9]Centro de Investigación Biomédica en Red Fisiopatología de la Obesidad y Nutrición (CIBERobn), 15782 Santiago de Compostela, Spain

[10]Department of Neurochemistry and Neuropharmacology, IIBB–CSIC–IDIBAPS, 08036 Barcelona, Spain

[11]Centro de Investigación Biomédica en Red de Salud Mental (CIBERSAM), 08036, Barcelona, Spain

SUMMARY

Mitofusin 2 (Mfn2) plays critical roles in both mitochondrial fusion and the establishment of mitochondria-endoplasmic reticulum (ER) interactions. Hypothalamic ER stress has emerged as a causative factor for the development of leptin resistance, but the underlying mechanisms are

Corresponding author: Marc Claret, Diabetes and Obesity Research Laboratory, Institut d'Investigacions Biomèdiques August Pi i Sunyer (IDIBAPS), Centre Esther Koplowitz, C/Rosselló 149-153, 5th floor, 08036 Barcelona, Spain. Phone: +34 932275400-4552. Fax: +34 933129409. mclaret@clinic.ub.es.

largely unknown. Here we show that mitochondria-ER contacts in anorexigenic pro-opiomelanocortin (POMC) neurons in the hypothalamus are decreased in diet-induced obesity. POMC-specific ablation of Mfn2 resulted in loss of mitochondria-ER contacts, defective POMC processing, ER stress-induced leptin resistance, hyperphagia, reduced energy expenditure and obesity. Pharmacological relieve of hypothalamic ER stress reversed these metabolic alterations. Our data establishes Mfn2 in POMC neurons as an essential regulator of systemic energy balance by fine-tuning the mitochondrial-ER axis homeostasis and function. This previously unrecognized role for Mfn2 argues for a crucial involvement in mediating ER stress-induced leptin resistance.

INTRODUCTION

The mediobasal hypothalamus is a critical area of the central nervous system implicated in the regulation of homeostatic functions. Specific populations of neurons in the arcuate nucleus (ARC) play fundamental roles in the regulation of energy balance (Williams and Elmquist, 2012). In particular, neurons co-expressing orexigenic neuropeptides agouti-related protein (AgRP) and neuropeptide Y (NPY) along with neurons co-expressing anorexigenic pro-opiomelanocortin (POMC) precursor and cocaine and amphetamine-related transcript (CART) have been extensively involved in the regulation of appetite, body weight and metabolism (Dieguez et al., 2011; Myers and Olson, 2012; Sisley and Sandoval, 2011; Williams and Elmquist, 2012).

A hallmark of obesity is leptin resistance, in which high circulating leptin levels are unable to promote its central anorexigenic effects (Bjorbaek, 2009). POMC neurons are primary targets of leptin in the hypothalamus and evidence suggests that alterations in this subset of neurons may mediate the development of hypothalamic leptin resistance (Bjorbaek, 2009; Diano et al., 2011; Gamber et al., 2012). Recent data demonstrate that enhanced hypothalamic endoplasmic reticulum (ER) stress and activation of the unfolded protein response (UPR) play a primary pathogenic role in leptin resistance development. For example, both diet-induced and genetic models of obesity have been associated with increased ER stress in the hypothalamus (Ozcan et al., 2009; Won et al., 2009; Zhang et al., 2008). Pharmacological or genetic ER stress induction causes hypothalamic leptin resistance and, consequently, increased appetite and obesity (Hosoi et al., 2008; Ozcan et al., 2009; Won et al., 2009; Zhang et al., 2008). Chemical chaperones relieve hypothalamic ER stress and act as leptin sensitizers, reducing food intake and body weight (Ozcan et al., 2009; Won et al., 2009; Zhang et al., 2008). Despite the strong link between ER stress and leptin resistance in the hypothalamus, the cellular and molecular determinants involved remain elusive.

The ER and mitochondria form contacts that support essential structural and functional interorganelle communication, a process that is partially modulated by mitochondrial fusion and fission (Rowland and Voeltz, 2012). Recent evidences indicate that Mitofusin 2 (Mfn2), a ubiquitously expressed mitochondrial transmembrane dynamin-like GTPase protein, plays fundamental roles in both mitochondrial fusion (Chen et al., 2003) and the establishment of mitochondria-ER interactions (de Brito and Scorrano, 2008). Intriguingly, mitochondrial and ER dysfunctions have been associated with the development of metabolic alterations and recent data suggest a key role for Mfn2 in the pathophysiology of obesity and type-2 diabetes in both humans and rodents (Bach et al., 2005; Bach et al., 2003; Hernandez-Alvarez et al., 2009; Hernandez-Alvarez et al., 2010; Sebastian et al., 2012).

These evidences encouraged us to hypothesize that Mfn2 in POMC neurons may be a molecular link between ER stress and leptin resistance in the hypothalamus. Here we provide evidence that mitochondrial dynamics and mitochondria-ER interactions in POMC neurons are altered in diet-induced obesity (DIO). Our data also indicate that Mfn2

deficiency in this population of neurons causes loss of mitochondria-ER contacts, ER stress, leptin resistance and reduced α-melanocyte stimulating hormone (α-MSH) production, leading to severe obesity. These results unravel an unexpected role for Mfn2 in the regulation of POMC neuronal function and hypothalamic ER stress to appropriately regulate whole-body energy balance.

RESULTS

Mitochondrial network and mitochondria-ER contacts in POMC neurons are altered in DIO

The cellular adaptations to fluctuations in nutrient availability involve the regulation of mitochondrial function, a process that is intimately associated with changes in mitochondrial dynamics and mitochondria-ER interactions (Baltzer et al., 2010; Mandl et al., 2009; Youle and van der Bliek, 2012). We assessed potential alterations in POMC neuron mitochondrial network complexity caused by energy excess in DIO mice using confocal microscopy. Aspect ratio (AR) and form factor (FF), parameters associated with mitochondria length and branching respectively, were decreased in POMC neurons from DIO mice when compared to lean controls (Figure 1A, 1B and Figure S1A, S1B). The positive correlation between mitochondria AR and FF in POMC neurons from lean mice was lost in DIO mice (Figure 1C). To further examine the effects of nutrient excess in POMC neurons, we conducted electron microscopy (EM) analysis. As previously described, mitochondrial density in POMC neurons from DIO mice was increased (Diano et al., 2011; data not shown). Interestingly, DIO mice showed a significant reduction in the number of mitochondria-ER contacts in POMC neurons when compared to lean controls (Figure 1D and 1E). Collectively, these results indicate that both mitochondrial network complexity and their association to ER in POMC neurons are altered in DIO mice.

Reduced *Mfn2* expression in the hypothalamus precedes the onset of obesity and its overexpression ameliorates the DIO phenotype

A candidate protein to mediate the alterations in mitochondria-ER contacts and mitochondrial network observed in DIO mice is Mfn2. To initially assess this, we conducted a time-course study and analyzed the expression of genes implicated in mitochondrial dynamics in the hypothalamus of lean and DIO mice at different time-points. While four days of high-fat diet did not cause changes in body weight (Figure 1F), hypothalamic *Mfn2* expression was already down-regulated (Figure 1G). Reduced *Mfn2* expression in the hypothalamus was observed throughout the study (Figure 1G). Expression of mitofusin 1 (*Mfn1*), optic atrophy 1 (*Opa1*), dynamin-related protein 1 (*Drp1*) and mitochondrial fission 1 (*Fis1*) remained unchanged (Figure S1C–F).

Next, we assessed whether adenovirus-mediated overexpression of Mfn2 in the ARC of DIO mice was able to improve their metabolic alterations. Localization studies showed correct delivery of the adenovirus (Figure 2A). Mfn2 overexpression (Figure 2B) in the ARC of DIO mice resulted in reduced body weight (Figure 2C), adiposity (Figure 2D) and plasma leptin levels (Figure 2E). This was associated with diminished food intake (Figure 2F) and increased interscapular surface temperature adjacent to brown adipose tissue (BAT) (Figure 2G). Consistent with this, the expression of BAT thermogenic marker uncoupling protein 1 (*Ucp-1*) was upregulated (Figure 2H) while the trend in hypothalamic neuropeptide expression was congruent with increased anorexigenic output (Figure 2I). Remarkably, Mfn2 overexpression in the ARC attenuated the hypothalamic DIO-induced expression of ER stress markers such as *Bip*, CCAAT/enhancer-binding protein-homologous protein (*Chop*), spliced form of X box binding protein 1 (*Xbp1s*), activating transcription factor 4 (*Atf4*) and 6 (*Atf6*) (Figure 2J).

Together, these results suggest that Mfn2 in the hypothalamus may underlie the metabolic alterations of DIO mice, and hence it can be a relevant protein implicated in the central regulation of energy balance.

Generation of mice lacking Mfn2 in POMC neurons

Mfn2 immunoreactivity was widely observed in the ARC including POMC neurons (Figure S2A). To explore the role of Mfn2 in POMC neurons upon the regulation of whole-body energy homeostasis, we generated POMC neuron specific Mfn2 knockout mice (*POMCMfn2KO*). We confirmed tissue-specific recombination of the Mfn2 floxed allele in the hypothalamus (Figure S2B). We also detected reduction in *Mfn2* gene expression, but not in other mitochondrial dynamics genes in the hypothalamus (Figure S2C). The POMC promoter also drives *cre* recombinase expression in corticotrophs and melanotrophs, so we examined the integrity and functionality of the pituitary-adrenal axis. Expression of pituitary genes *Pomc*, T box transcription factor (*Tpit*), corticotrophin releasing hormone receptor 1 (*Crhr1*), pituitary-specific transcription factor 1 (*Pit1*), growth hormone (*Gh*) and thyroid-stimulating hormone beta-chain (*Tshβ*) were unaltered (Figure S2D). Plasma corticosterone levels were equivalent between control and *POMCMfn2KO* mice under basal conditions, and the stress response was preserved (Figure S2E). Epinephrine, norepinephrine and dopamine concentrations were normal in mutant mice (Figure S2F–H). These results indicate that deletion of Mfn2 in pituitary cells does not cause defects in the pituitary-adrenal axis.

Anatomical assessment of POMC neurons throughout the ARC revealed no alterations in neuronal population size, distribution or somatic area (Figure S2I–K), indicating that Mfn2 deficiency did not alter POMC neuron differentiation and/or survival.

Deletion of Mfn2 in POMC neurons causes severe obesity

Male *POMCMfn2KO* mice exhibited a marked obese phenotype that was significant by 7 weeks of age onwards (Figure 3A). *POMCMfn2KO* mice were hyperphagic both under *ad libitum* conditions (Figure 3B) and after a fast-refeeding test (Figure 3C) suggesting impaired satiety mechanisms. Female mutant mice displayed a similar phenotype (data not shown), so we undertook subsequent studies in male mice.

Altered energy homeostasis in *POMCMfn2KO* mice was further demonstrated by reduced oxygen consumption and energy expenditure (Figure 3D and 3E). Given that energy expenditure includes physical activity and thermogenesis, we undertook studies to measure these parameters. Ambulation activity was unchanged (control: 6016±453 counts/24h; *POMCMfn2KO*: 7174±567 counts/24h; n=7–8, NS). However, interscapular temperature adjacent to BAT was reduced in mutant mice (Figure 3F and 3G). Consistently, mRNA expression of BAT thermogenic markers *Ucp1* and peroxisome proliferator-activated receptor gamma coactivator 1-alpha (*Pgc1α*) were decreased in *POMCMfn2KO* mice (Figure 3H). Obesity is closely associated with alterations in glucose metabolism. As expected, 12-week old mutant mice exhibited hyperglycemia, hyperinsulinemia, glucose intolerance and insulin resistance (data not shown). Altogether, these results demonstrate that the obese phenotype observed in *POMCMfn2KO* mice is due to hyperphagia and reduced activity of the thermogenic program.

To assess the specificity of the metabolic consequences caused by Mfn2 deficiency in POMC neurons, we characterized mice lacking Mfn1 (a closely related mitofusin protein) in the same population of neurons (*POMCMfn1KO*). Appropriate deletion of Mfn1 was assessed by the recombination event and gene expression analysis (data not shown and Figure S3A). The pituitary-adrenal axis function was preserved as suggested by unaltered

expression of pituitary genes (Figure S3B), plasma corticosterone (Figure S3C) and catecholamines (Figure S3D–F). In contrast to *POMCMfn2KO* mice, energy balance parameters such as body weight (Figure S3G), adiposity (Figure S3H), plasma leptin levels (Figure S3I) and feeding behavior (Figure S3J and S3K) were unaltered in *POMCMfn1KO* mice. Oxygen consumption (Figure S3L), energy expenditure (Figure S3M), interscapular temperature (Figure S3N) and 24h ambulation activity (data not shown) were comparable between mutant and control mice. Consistent with the lack of alterations in energy homeostasis, hypothalamic neuropeptide expression was unchanged (Figure S3O). These results demonstrate a specific role for Mfn2 in POMC neurons in the regulation of energy balance.

Loss of Mfn2 in POMC neurons leads to reduced POMC processing into α-MSH

To investigate the mechanisms underlying the hypothalamic phenotype of *POMCMfn2KO* mice, we assessed neuropeptide gene expression. While mRNA expression of *Agrp*, *Npy* and *Cart* exhibited no differences between genotypes and appropriate regulation according to the nutritional status (Figure 4A), *Pomc* mRNA in mutant mice was downregulated and insensitive to the fed/fasting transition (Figure 4A). Reduced fasting *Pomc* gene expression was also observed in 6-week old mutant mice (control: 100±7 % vs. *POMCMfn2KO*: 44±4 %; n=12–16, $P<0.0001$).

POMC is a prohormone that in the ARC undergoes posttranslational proteolysis by the sequential activity of different convertases to generate α-MSH, a key melanocortin system component implicated in energy homeostasis (Wardlaw, 2011). Hence, we measured POMC and α-MSH content in hypothalamic extracts from 6 and 12-week old control and *POMCMfn2KO* mice. Whereas total POMC content was increased in the hypothalamus from mutant mice (Figure 4B), α-MSH content was decreased by ~50–60% at both ages (Figure 4C). The α-MSH/POMC ratio, a measure of POMC precursor processing, was also decreased (Figure 4D). However, reduced α-MSH concentration did not seem to be the consequence of defective expression of processing enzymes, since mRNA levels of prohormone convertase 1 (*Pc1/3*), prohormone convertase 2 (*Pc2*), carboxypeptidase E (*Cpe*), α-amidating monooxygenase (*Pam*) and prolylcarboxypeptidase (*Prcp*) were either unchanged or regulated in opposite manner (Figure 4E and 4F).

α-MSH is released from POMC axonal terminals to the paraventricular nucleus (PVN) of the hypothalamus where exerts its anorexigenic actions. Thus, we examined α-MSH peptide expression in the PVN by immunohistochemistry and found a dramatic reduction of α-MSH staining in neuronal projections from mutant mice (Figure 4G and 4H).

To investigate whether the obese phenotype in *POMCMfn2KO* mice resulted from reduced α-MSH production, we assessed the anorectic effects of intracerebroventricular (i.c.v.) administration of this peptide. A daily single dose of α-MSH to *POMCMfn2KO* mice normalized food intake and markedly reduced body weight gain (Figure 4I and 4J). Collectively, our data suggest that deletion of Mfn2 in POMC neurons leads to reduced α-MSH concentration in the hypothalamus, being this defect the cause of the *POMCMfn2KO* obese phenotype.

POMCMfn2KO mice develop early-onset leptin resistance

The obese phenotype of *POMCMfn2KO* mice resulted from increased adiposity (Figure 5A). Consistently, plasma leptin levels were also elevated (Figure 5B), a scenario indicative of leptin resistance. To examine leptin action in *POMCMfn2KO* mice we performed a leptin sensitivity test. The anorectic effects of leptin were clearly detectable in 12-week old control mice. In contrast, the effect of this hormone was blunted in *POMCMfn2KO* mice suggesting

leptin resistance (Figure 5C and 5D). We next asked whether defective leptin sensitivity in *POMCMfn2KO* mice was a primary defect or secondary to the development of obesity. Thus, we assessed leptin sensitivity at 6 weeks of age when body weight (control: 22.1±0.3 g; *POMCMfn2KO*: 21.0±1.5 g; n=6, NS; Figure 3A) and adiposity (control: 13.7±0.8 %; *POMCMfn2KO*: 14.2±1.0 %; n=6, NS) were still unchanged. The anorectic effects of exogenous leptin were significantly attenuated in mice lacking Mfn2 in POMC neurons (Figure 5E and 5F; reduction in food intake vehicle vs. leptin: control 49±3 %, *POMCMfn2KO* 35±2 %; n=6, P=0.005). To confirm these findings we examined leptin signaling by double immunofluorescence analysis of phospho-Stat3 (pStat3) in POMC neurons. Leptin administration increased pStat3 in POMC neurons of control mice, but to a significantly lesser extent in POMC neurons from 6 week-old *POMCMfn2KO* mice (Figure 5G and 5H). Together, these results indicate that deletion of Mfn2 in POMC neurons leads to an early state of leptin resistance in the hypothalamus that is independent of obesity.

Deficiency of Mfn2 in POMC neurons alters mitochondrial morphology, mitochondria-ER contacts and induces ER stress

It has been shown that ER stress plays a key role in the development of leptin resistance and obesity (Ozcan et al., 2009; Zhang et al., 2008). Given that Mfn2 supports structural and functional communication between mitochondria and ER (de Brito and Scorrano, 2008) and that genetic loss of Mfn2 causes ER stress (Ngoh et al., 2012; Sebastian et al., 2012), we investigated whether deletion of Mfn2 in POMC neurons leads to alterations in mitochondria and ER homeostasis. Ultrastructure analysis by EM showed similar density of mitochondria related to cell size in POMC neurons from mutant mice (Figure 6A–C), concomitant with an increase in mitochondria coverage of the cell area (Figure 6D). This change was due to enlarged mitochondria (Figure 6E), which also presented altered shape (Figure 6F). Mitochondria from POMC neurons lacking Mfn2 also contained smaller and more rounded cristae (data not shown). Remarkably, while most mitochondria in control POMC neurons showed close interactions with ER, the number of mitochondria-ER contacts was significantly reduced in POMC neurons from *POMCMfn2KO* mice (Figure 6A, B and G). Similar results were observed in POMC neuron mitochondria from non-obese 6-weeks old mutant mice (Figure S4A and B), indicating that these alterations precede the onset of obesity. These results imply Mfn2 as a critical protein in the maintenance of mitochondria morphology and mitochondria-ER interactions in hypothalamic POMC neurons.

Next we conducted gene expression analysis of ER-stress markers in the hypothalamus. By 6 weeks of age we observed an emerging state of ER-stress in *POMCMfn2KO* mice, characterized by the upregulation of *Xbp1s* and *Atf4* (Figure 6H). By 12-weeks of age, the expression levels of *Bip*, *Chop*, *Xbp1s* and *Atf4* were significantly increased indicating overt ER-stress (Figure 6I). Consistently, protein expression analysis of ER-stress markers in the hypothalamus from *POMCMfn2KO* mice exhibited a similar pattern (Figure S4C and D). Altogether, these results suggest that inactivation of Mfn2 in POMC neurons leads to loss of mitochondria-ER interactions and primary ER stress.

Mfn2 deletion in POMC neurons alters mitochondrial respiratory capacity and enhances ROS production

Next we assessed whether loss of Mfn2 in POMC neurons altered mitochondrial respiratory capacity using high-resolution respirometry. The respiratory states Leak, oxidative phosphorylation due to the addition of complex I and complex I and II substrates in the presence of ADP (Oxphos I and Oxphos I+II) and maximum electron transport system capacity (ETSI+II) were significantly reduced in hypothalamic lysates from *POMCMfn2KO* mice (Figure S5A). Gene expression of Complex I NADH dehydrogenase [ubiquinone] 1 alpha subcomplex subunit 9 (*Ndufa9*) was reduced in the hypothalamus of mutant mice at

both 6 and 12 weeks of age (Figure S5B). Together, these results suggest impaired mitochondrial Complex I function.

Reduced activity of Complex I is associated with increased reactive oxygen species (ROS) production. Thus, we measured ROS levels in the hypothalamus by the assessment of protein carbonylation, a standard marker for oxidative stress. The level of carbonylated proteins was higher in hypothalamic lysates from *POMCMfn2KO* mice (Figure S5C). Expression of ROS detoxification enzymes Catalase (*Cat*), Glutathione peroxidase 1 (*Gpx-1*) and Superoxide dismutase 2 (*Sod2*) was significantly increased in the hypothalamus from mutant mice before and after the onset of obesity (Figure S5D and E). These results might reflect a compensatory mechanism aimed to reduce the excess of ROS generated.

Our data show specific mitochondrial function disturbances and enhanced ROS production in the hypothalamus of *POMCMfn2KO* mice. Increased ROS levels in the hypothalamus causes reduced food intake and body weight gain in rodents (Diano et al., 2011; Gyengesi et al., 2012), so it is unlikely that excessive ROS generation contributes to the obesogenic phenotype of *POMCMfn2KO* mice. Nevertheless, we undertook experiments to assess this hypothesis by i.c.v. injection of the ROS scavenger honokiol. Consistent with previous results (Diano et al., 2011), central honokiol administration significantly increased food intake and body weight gain in control mice and these effects were further magnified in mutant mice (Figure S5F and G), indicating that enhanced ROS generation in the hypothalamus is not the cause of the obesogenic phenotype of these animals.

Inhibition of hypothalamic ER stress by chemical chaperone treatment reverses the obesogenic phenotype of *POMCMfn2KO* mice

Chemical chaperones, such as 4-phenyl butyric acid (4-PBA) or tauroursodeoxycholic acid (TUDCA), are able to relieve ER stress and improve ER function in different tissues including the hypothalamus (Ozcan et al., 2009; Zhang et al., 2008). To test whether the metabolic defects observed in *POMCMfn2KO* mice resulted from hypothalamic ER stress, we conducted i.c.v. injections of either 4-PBA or TUDCA to control and *POMCMfn2KO* mice. 4-PBA administration did not change food intake or body weight gain in control mice (Figure 7A and 7B). In contrast, this treatment completely normalized food intake and body weight in mutant mice (Figure 7A and 7B). Consistent with this, adiposity (Figure 7C) and plasma leptin levels (Figure 7D) were restored in *POMCMfn2KO* mice treated with 4-PBA. Chaperone treatment also normalized the expression of *Xbp1s, Chop, Atf4* and PERK phosphorylation in the hypothalamus of mutant mice, indicating ER stress relieve (Figure 7E and data not shown). Remarkably, 4-PBA treatment normalized *Pomc* mRNA expression as well as the content of POMC precursor, α-MSH and α-MSH/POMC ratio in the hypothalamus from *POMCMfn2KO* mice (Figure 7F–I). α-MSH immunoreactivity in the PVN was also regained in mutant mice after 4-PBA administration (Figure 7J and 7K). The beneficial effects of 4-PBA were not associated with reduced hypothalamic levels of carbonylated proteins (Figure S5H), demonstrating that the normalization of the phenotype was not the consequence of changes in hypothalamic ROS. Central TUDCA treatment essentially reproduced the effects of 4-PBA by significantly improving the metabolic alterations of *POMCMfn2KO*, although it was unable to completely restore their phenotype (Figure S6A–K). Collectively, these results indicate that i.c.v. treatment with two structurally unrelated chemical chaperones is able to recover the physiological and molecular alterations found in *POMCMfn2KO* mice, suggesting that these are the consequence of hypothalamic ER stress.

DISCUSSION

Here we show that Mfn2 in POMC neurons is an essential regulator of whole-body energy balance. We suggest a model whereby disruption of proper mitochondrial-ER homeostasis through Mfn2 deletion in POMC neurons leads to primary ER stress, defective α-MSH processing, leptin resistance and obesity. Thus, our data support the notion that Mfn2 is a molecular determinant implicated in the development of ER stress-induced leptin resistance. ER and mitochondria are able to sense nutrient fluctuations and integrate coordinated responses aimed to maintain cell homeostasis (Baltzer et al., 2010; Youle and van der Bliek, 2012). This is achieved through the establishment of contact sites between both organelles that participate in essential bidirectional communication processes (Rowland and Voeltz, 2012). Given that mitochondrial morphology is continuously changed through fusion and fission events, a tight coordination between mitochondrial dynamics and interorganelle interactions is crucial. Mfn2 has been extensively implicated in mitochondrial fusion (Zorzano et al., 2010), but recent data also demonstrate a key role for Mfn2 tethering ER with mitochondria (de Brito and Scorrano, 2008). This dual role of Mfn2 is unique and makes it a good candidate to coordinate ER and mitochondrial functions, especially those modulated by metabolic stress. In agreement with this, we found that nutrient excess in DIO mice altered the mitochondrial network complexity and reduced the number of mitochondrial-ER contacts in POMC neurons. This was correlated with specific downregulation of *Mfn2* expression in the hypothalamus. Overexpression of Mfn2 in the ARC of DIO mice ameliorated their metabolic defects, suggesting a causative role for Mfn2 in the development of metabolic alterations under nutrient excess conditions. In contrast, high-fat feeding stimulated a mitochondrial fusion-like process in AgRP neurons (Dietrich et al., 2013) suggesting cell-type-specific roles for Mfn2 upon mitochondrial dynamics. Collectively, this data support the current idea that mitochondrial fusion is regulated by energy demand and stress (Youle and van der Bliek, 2012), and suggest that Mfn2 is a key determinant of a molecular pathway that integrates nutritional changes with the mitochondria-ER axis to adapt and maximize the function of this system.

Consistent with a key role for Mfn2 in metabolic regulation, deletion of Mfn2 in POMC neurons caused a dramatic obese phenotype characterized by increased adiposity, hyperphagia and reduced energy expenditure. ARC POMC neurons are major targets of leptin action, stimulating POMC transcription through the Jak2-Stat3 pathway and triggering the release of the anorexigenic neuropeptide α-MSH from POMC axon terminals (Kitamura et al., 2006; Munzberg et al., 2003). In line with this, *POMCMfn2KO* mice exhibited attenuated leptin effects and reduced pStat3 staining in POMC neurons before the onset of obesity. In addition, *Pomc* mRNA expression was reduced and unresponsive to the fed/fasting transition in *POMCMfn2KO* mice. Together, our data indicate that loss of Mfn2 in POMC neurons cause primary leptin resistance independent of obesity.

Hypothalamic ER stress has recently emerged as a causal factor in the development of central leptin resistance (Hosoi et al., 2008; Ozcan et al., 2009; Won et al., 2009; Zhang et al., 2008). Given the cellular localization and function of Mfn2, we reasoned that this protein could represent a molecular link between hypothalamic ER stress and leptin resistance. Ultrastructural analysis of POMC neurons lacking Mfn2 revealed spherical and enlarged mitochondria, a morphology that is in line with previous studies (Chen et al., 2007; Lee et al., 2012; Papanicolaou et al., 2011). Remarkably, we observed a reduction in mitochondria-ER contacts in POMC neurons from *POMCMfn2KO* obese mice. The extension of this loss of contact sites was strikingly similar to those observed in DIO mice, suggesting that defective mitochondria-ER contacts may underlie leptin resistance and obesity development. Furthermore, hypothalamic gene and protein expression analysis showed incipient upregulation of ER stress markers in non-obese *POMCMfn2KO* mice, a

defect that was further enhanced in adult mutant mice. Deletion of Mfn2 in AgRP neurons did not lead to alterations in mitochondria-ER contacts (Dietrich et al., 2013), further indicating divergent roles for Mfn2 in a cell-type specific manner.

The neurobiological cause of hypothalamic ER stress-induced leptin resistance is still unknown, but likely due to a combination of defects. For example, *in vitro* and *in vivo* data indicate that ER stress and the activation of the UPR signaling network directly block leptin signaling by reducing pStat3 levels (Ozcan et al., 2009). Consistently, *POMCMfn2KO* mice displayed reduced pStat3 staining in POMC neurons. Furthermore, the ER is involved in the synthesis, folding and transport of secretory proteins (Rowland and Voeltz, 2012). It is plausible that dysfunctional ER may interfere with proper synthesis and release of key neuropeptides that mediate the anorectic effects of leptin, thereby altering whole-body energy balance. Hence, ER stress in POMC neurons could result in defective POMC processing and/or α-MSH production. We observed that, although POMC protein was increased likely as a consequence of compensatory mechanisms, total α-MSH content and processing rate was reduced in mutant mice. POMC processing alterations were not due to reduced expression of convertases. In fact, upregulation of some of these convertases and downregulation of α-MSH degrading enzyme *Prcp* (Wallingford et al., 2009) was observed, probably as a molecular adaptation to maintain the appropriate anorexigenic tone. Defective POMC processing was observed before the onset of obesity suggesting that this chain of events precede, and are likely the cause, of the development of obesity in *POMCMfn2KO* mice.

We further demonstrated that ER stress was the underlying cause of the metabolic phenotype of *POMCMfn2KO* mice through a rescue experiment. I.c.v. administration of two structurally unrelated chemical chaperones, such as 4-PBA or TUDCA, was able to fully recover or improve to great extent the physiological and molecular alterations of *POMCMfn2KO* mice. These results support the notion that loss of Mfn2 in POMC neurons cause abnormal hypothalamic ER homeostasis and function, leading to defective POMC neuropeptide production and processing. Our data is consistent with reports indicating that deletion of Mfn2 causes ER stress both *in vitro* and *in vivo* (Ngoh et al., 2012; Sebastian et al., 2012).

Recent studies suggest that neuronal Mfn2 deficiency or deleterious mutations promote neuronal and/or axonal degeneration, although direct assessment of defective axonal growth is lacking in some of these reports (Chen et al., 2007; Lee et al., 2012; Misko et al., 2012; Pham et al., 2012). *POMCMfn2KO* mice exhibited a dramatic reduction in α-MSH in neuronal projections to the PVN without alterations in POMC neuron number. This could be interpreted as evidence supporting compromised axon integrity, but the fact that 4-PBA and TUDCA treatment was able to restore α-MSH immunoreactivity in the PVN argues against this hypothesis. Similarly, loss of Mfn2 in AgRP neurons did not cause axon degeneration (Dietrich et al., 2013). Collectively, these evidences suggest cell-specific functions of Mfn2 in relation to neuronal survival and axon integrity.

Mfn1 and Mfn2 are highly homologous proteins, but a number of studies using conditional mouse mutants have shown that they are not entirely redundant (Chen et al., 2007; Lee et al., 2012; Papanicolaou et al., 2011; Papanicolaou et al., 2012; Pham et al., 2012). Our data further demonstrate specific and non-overlapping functions for Mfn1 and Mfn2, as deletion of Mfn1 in POMC neurons did not cause alterations in energy balance. It is now generally recognized that Mfn1 is mainly implicated in mitochondrial fusion, whereas Mfn2 could mediate additional functions such as mitochondria-ER tethering and mitochondrial transport. Our data indicate a main role for Mfn2 in POMC neurons upon ER homeostasis maintenance.

Defective ER and mitochondrial function has been extensively associated with metabolic disorders. In previous studies, we have demonstrated the significance of Mfn2 in skeletal muscle and liver in the pathophysiology of obesity and type-2 diabetes in both humans and rodents (Bach et al., 2005; Bach et al., 2003; Hernandez-Alvarez et al., 2009; Hernandez-Alvarez et al., 2010; Sebastian et al., 2012). Here we further expanded this knowledge to hypothalamic POMC neurons, a key population of neurons implicated in whole-body energy homeostasis, and provided evidence for a causative link between nutrient excess and alterations in mitochondrial dynamics, mitochondria-ER interactions and Mfn2 expression. Importantly, our data also established Mfn2 in POMC neurons as an essential regulator of systemic energy balance by fine-tuning the mitochondrial-ER axis homeostasis and function. This previously unrecognized role for Mfn2 argues for a critical involvement in mediating ER stress-induced leptin resistance.

EXPERIMENTAL PROCEDURES

Mice and diets

C57BL/6 mice were purchased from Harlan Europe. The generation of *POMC-Cre* mice has been previously reported (Xu et al., 2005). *Mfn1*$^{loxp/loxp}$ and *Mfn2*$^{loxp/loxp}$ mice were provided by Dr. David C Chan (Chen et al., 2007) through the Mutant Mouse Regional Resource Center. To generate POMC-specific Mfn1 and Mfn2 knock-out mice (*POMCMfn1KO* and *POMCMfn2KO*, respectively), *POMC-Cre* mice were crossed with *Mfn1*$^{loxp/loxp}$ or *Mfn2*$^{loxp/loxp}$ mice. Colonies were maintained by breeding *POMC-cre; loxp/loxp* mice with *loxp/loxp* mice. To generate mice expressing GFP in cells harboring the deletion event, mice were intercrossed with Z/EG mice (Novak et al., 2000). Mice were maintained on a 12:12h light–dark cycle with free access to water and standard chow (Harlan Research Laboratories) or high-fat diet (45% Kcal fat; Research Diets) for 12 weeks (starting at 6 weeks of age). I*n vivo* studies were performed with approval of the University of Barcelona Ethics Committee, complying with current Spanish and European legislation.

Physiological measurements

Body weights were weekly determined. Blood samples were collected via tail vein or trunk bleeds using a capillary collection system (Sarstedt). Blood glucose was measured using a Glucometer (Arkray). Plasma insulin and leptin were analyzed by ELISA (Crystal Chem Inc) and corticosterone by enzyme immunoassay (IDS). Catecholamines were measured by ELISA (Labor Diagnostika Nord). Glucose tolerance tests were performed on overnight fasted mice. D-glucose (2g/kg) was injected intraperitoneally (i.p.) and blood glucose determined at the indicated time points. Insulin sensitivity tests were performed on 4h food-deprived mice. Insulin (0.4 IU/kg) was injected i.p. and blood glucose determined at the indicated time points.

Body composition, thermal imaging and indirect calorimetry

Whole-body composition was measured using NMR imaging (EchoMRI). Heat production was visualized using a high-resolution infrared camera (FLIR Systems) as previously described (Czyzyk et al., 2012). Indirect calorimetry was assessed using a TSE LabMaster modular research platform (TSE Systems) as previously described (Czyzyk et al., 2012).

Feeding studies and leptin sensitivity tests

Mice were singly housed and acclimatized for 1-week prior to study. Food intake was measured for 5 consecutive days. For fast-refeeding studies, mice were overnight fasted and refeed with a preweighed amount of food. Food intake was measured at the indicated time points. For leptin sensitivity tests, mice were acclimatized by subjecting them to handling

and sham injections. Leptin tests were conducted in a crossover fashion. Twelve-week old control and *POMCMfn2KO* mice were i.p. injected with either 1.5 μg/g of mouse leptin (R&D Systems) or vehicle twice a day (1h before lights-out (7 p.m.) and at 8.00 a.m.) for 3 consecutive days. Six-week old control and *POMCMfn2KO* mice were submitted to an acute leptin test to assure similar body weights during the protocol. I.p. administration of either 5 μg/g of leptin (R&D Systems) or vehicle 1h before lights-out was performed. Food intake and body weights were recorded daily.

Quantitative RT-PCR (qPCR)

Hypothalami and pituitaries were harvested and immediately frozen in liquid nitrogen. mRNA was isolated using Trizol (Invitrogen). Retrotranscription and quantitative RT-PCR (qPCR) was performed as previously described (Claret et al., 2007). Proprietary Taqman Gene Expression assay FAM/TAMRA primers used (Applied Biosystems) are detailed in Extended Experimental Procedures. mRNA levels were measured using the ABI Prism 7900 HT system (Applied Biosystems).

Electron microscopy and mitochondrial analysis

Electron microscopy and analysis was performed as described (Dietrich et al., 2013). Detailed protocols are provided in Extended Experimental Procedures.

Hypothalamic POMC and α-MSH protein content

Hypothalami were sonicated in 500 μl of 0.1N HCl solution. Lysates were centrifuged and supernatants used for the quantification of POMC (Uscn Life Science) and α-MSH (Phoenix Pharmaceuticals) by ELISA. Protein concentration was determined by Bradford.

Hypothalamic immunohistochemistry

Brains were processed and immunohistochemistry conducted as described (Claret et al., 2007; Claret et al., 2011). Antibodies used are detailed in Extended Experimental Procedures. Imaging was performed using a Leica DMI 6000B microscope. α-MSH integrated density after image skeletonization was calculated using ImageJ software.

POMC neuron count and area

The distribution and number of POMC neurons were determined as described (Claret et al., 2007). Average somatic area was analyzed in >500 POMC neurons (n=3 mice/genotype). The area occupied by POMC neurons was manually scored using Image J software.

Quantification of leptin-induced pSTAT3 in POMC neurons

Six-week old male *POMCZ/EG* and *POMCMfn2KOZ/EG* mice were injected i.p. with either saline or 5 μg/g mouse leptin (R&D Systems). Mice were transcardially perfused 45 min after injection and brains processed for pStat3 immunohistochemistry (1:1,000, Cell Signaling). Double GFP and pStat3 labeling was determined in matched sections (n=3 mice/group).

Mitochondrial network complexity analysis in POMC neurons

Mitochondrial morphology and network complexity in POMC neurons was assessed by confocal microscopy and computer-assisted analysis. Detailed methodology is provided in Extended Experimental Procedures.

I.c.v. cannulation and treatments

I.c.v. surgery was performed as previously described (Al-Qassab et al., 2009). Detailed protocols and treatments are provided in Extended Experimental Procedures.

Statistics

Data are expressed as mean ± SEM. *P* values were calculated using unpaired Student's t test or one-way ANOVA with post-hoc Tukey tests as appropriate. $P \leq 0.05$ was considered significant.

Supplementary Material

Refer to Web version on PubMed Central for supplementary material.

Acknowledgments

We are grateful to Dr Gregory S Barsh (Stanford University) for providing *Pomc-cre* mice, Dr Maria Calvo and Anna Bosch from the Confocal microscopy unit (SCT-UB), Mercè Monfar (UPV-CBATEG) and members from the Diabetes and Obesity Lab. This work has been supported by: RecerCaixa Grant 2010ACUP_00275 (MC); EFSD/Lilly Fellowship Award (MC); Ministerio de Ciencia e Innovación (MICINN), Instituto de Salud Carlos III (ISCIII) Grant PI10/01074 (MC); MICINN Grant SAF2010-19527 (RG); Ministerio de Economia y Competitividad (MINECO) Grant BFU2012-35255 (RN); Xunta de Galicia Grant EM2012/039 and 2012-CP069 (RN); CIBERobn (RN); European Community's Seventh Framework Programme Grant ERC-2011-StG-OBESITY53-281408 (RN); MINECO Grant SAF2008-03803 (AZ); Generalitat de Catalunya Grant 2009SGR915 (AZ); CIBERDEM (AZ); INTERREG IV-B-SUDOE-FEDER (DIOMED, SOE1/P1/E178) (AZ); European Commission Seventh Framework Programme (FP7), MITIN Grant HEALTH-F4-2008-223450 (AZ); MICINN Grant BFU2011- 24679 (PM G-R); ISCIII Grant PI10/00290 (AB). TLH and MOD are supported by NIH (DP1DK006850, R01AG040236, P01NS062686), American Diabetes Association, Helmholtz society (ICEMED) and by Conselho Nacional de Desenvolvimento Científico e Tecnológico (401476/2012-0, Brazil). MS is a recipient of an undergraduate grant from the University of Barcelona. MC is a recipient of a Miguel Servet contract (CP09/00233) from MICINN-ISCIII. PMG-R is a recipient of a Ramon y Cajal contract (RYC-2009-05158) from MICINN. Some of these grants are co-financed by the European Regional Development Fund "A way to build Europe". This work was carried out in part at the Esther Koplowitz Centre, Barcelona.

References

Al-Qassab H, Smith MA, Irvine EE, Guillermet-Guibert J, Claret M, Choudhury AI, Selman C, Piipari K, Clements M, Lingard S, et al. Dominant role of the p110beta isoform of PI3K over p110alpha in energy homeostasis regulation by POMC and AgRP neurons. Cell Metab. 2009; 10:343–354. [PubMed: 19883613]

Bach D, Naon D, Pich S, Soriano FX, Vega N, Rieusset J, Laville M, Guillet C, Boirie Y, Wallberg-Henriksson H, et al. Expression of Mfn2, the Charcot-Marie-Tooth neuropathy type 2A gene, in human skeletal muscle: effects of type 2 diabetes, obesity, weight loss, and the regulatory role of tumor necrosis factor alpha and interleukin-6. Diabetes. 2005; 54:2685–2693. [PubMed: 16123358]

Bach D, Pich S, Soriano FX, Vega N, Baumgartner B, Oriola J, Daugaard JR, Lloberas J, Camps M, Zierath JR, et al. Mitofusin-2 determines mitochondrial network architecture and mitochondrial metabolism. A novel regulatory mechanism altered in obesity. J Biol Chem. 2003; 278:17190–17197. [PubMed: 12598526]

Baltzer C, Tiefenbock SK, Frei C. Mitochondria in response to nutrients and nutrient-sensitive pathways. Mitochondrion. 2010; 10:589–597. [PubMed: 20696279]

Bjorbaek C. Central leptin receptor action and resistance in obesity. J Investig Med. 2009; 57:789–794.

Chen H, Detmer SA, Ewald AJ, Griffin EE, Fraser SE, Chan DC. Mitofusins Mfn1 and Mfn2 coordinately regulate mitochondrial fusion and are essential for embryonic development. The Journal of cell biology. 2003; 160:189–200. [PubMed: 12527753]

Chen H, McCaffery JM, Chan DC. Mitochondrial fusion protects against neurodegeneration in the cerebellum. Cell. 2007; 130:548–562. [PubMed: 17693261]

Claret M, Smith MA, Batterham RL, Selman C, Choudhury AI, Fryer LG, Clements M, Al-Qassab H, Heffron H, Xu AW, et al. AMPK is essential for energy homeostasis regulation and glucose sensing by POMC and AgRP neurons. J Clin Invest. 2007; 117:2325–2336. [PubMed: 17671657]

Claret M, Smith MA, Knauf C, Al-Qassab H, Woods A, Heslegrave A, Piipari K, Emmanuel JJ, Colom A, Valet P, et al. Deletion of Lkb1 in pro-opiomelanocortin neurons impairs peripheral glucose homeostasis in mice. Diabetes. 2011; 60:735–745. [PubMed: 21266325]

Czyzyk TA, Romero-Pico A, Pintar J, McKinzie JH, Tschop MH, Statnick MA, Nogueiras R. Mice lacking delta-opioid receptors resist the development of diet-induced obesity. FASEB J. 2012; 26:3483–3492. [PubMed: 22593549]

de Brito OM, Scorrano L. Mitofusin 2 tethers endoplasmic reticulum to mitochondria. Nature. 2008; 456:605–610. [PubMed: 19052620]

Diano S, Liu ZW, Jeong JK, Dietrich MO, Ruan HB, Kim E, Suyama S, Kelly K, Gyengesi E, Arbiser JL, et al. Peroxisome proliferation-associated control of reactive oxygen species sets melanocortin tone and feeding in diet-induced obesity. Nat Med. 2011; 17:1121–1127. [PubMed: 21873987]

Dieguez C, Vazquez MJ, Romero A, Lopez M, Nogueiras R. Hypothalamic control of lipid metabolism: focus on leptin, ghrelin and melanocortins. Neuroendocrinology. 2011; 94:1–11. [PubMed: 21576929]

Dietrich M, Liu Z-W, Horvath TL. Mitochondrial dynamics controlled by mitofusins regulate Agrp neuronal activity and diet-induced obesity. Cell. 2013

Gamber KM, Huo L, Ha S, Hairston JE, Greeley S, Bjorbaek C. Over-expression of leptin receptors in hypothalamic POMC neurons increases susceptibility to diet-induced obesity. PloS one. 2012; 7:e30485. [PubMed: 22276206]

Gyengesi E, Paxinos G, Andrews ZB. Oxidative Stress in the Hypothalamus: the Importance of Calcium Signaling and Mitochondrial ROS in Body Weight Regulation. Curr Neuropharmacol. 2012; 10:344–353. [PubMed: 23730258]

Hernandez-Alvarez MI, Chiellini C, Manco M, Naon D, Liesa M, Palacin M, Mingrone G, Zorzano A. Genes involved in mitochondrial biogenesis/function are induced in response to bilio-pancreatic diversion in morbidly obese individuals with normal glucose tolerance but not in type 2 diabetic patients. Diabetologia. 2009; 52:1618–1627. [PubMed: 19504086]

Hernandez-Alvarez MI, Thabit H, Burns N, Shah S, Brema I, Hatunic M, Finucane F, Liesa M, Chiellini C, Naon D, et al. Subjects with early-onset type 2 diabetes show defective activation of the skeletal muscle PGC-1{alpha}/Mitofusin-2 regulatory pathway in response to physical activity. Diabetes care. 2010; 33:645–651. [PubMed: 20032281]

Hosoi T, Sasaki M, Miyahara T, Hashimoto C, Matsuo S, Yoshii M, Ozawa K. Endoplasmic reticulum stress induces leptin resistance. Mol Pharmacol. 2008; 74:1610–1619. [PubMed: 18755873]

Kitamura T, Feng Y, Kitamura YI, Chua SC Jr, Xu AW, Barsh GS, Rossetti L, Accili D. Forkhead protein FoxO1 mediates Agrp-dependent effects of leptin on food intake. Nat Med. 2006; 12:534–540. [PubMed: 16604086]

Lee S, Sterky FH, Mourier A, Terzioglu M, Cullheim S, Olson L, Larsson NG. Mitofusin 2 is necessary for striatal axonal projections of midbrain dopamine neurons. Hum Mol Genet. 2012; 21:4827–4835. [PubMed: 22914740]

Mandl J, Meszaros T, Banhegyi G, Hunyady L, Csala M. Endoplasmic reticulum: nutrient sensor in physiology and pathology. Trends Endocrinol Metab. 2009; 20:194–201. [PubMed: 19349192]

Misko AL, Sasaki Y, Tuck E, Milbrandt J, Baloh RH. Mitofusin2 mutations disrupt axonal mitochondrial positioning and promote axon degeneration. J Neurosci. 2012; 32:4145–4155. [PubMed: 22442078]

Munzberg H, Huo L, Nillni EA, Hollenberg AN, Bjorbaek C. Role of signal transducer and activator of transcription 3 in regulation of hypothalamic proopiomelanocortin gene expression by leptin. Endocrinology. 2003; 144:2121–2131. [PubMed: 12697721]

Myers MG Jr, Olson DP. Central nervous system control of metabolism. Nature. 2012; 491:357–363. [PubMed: 23151578]

Ngoh GA, Papanicolaou KN, Walsh K. Loss of mitofusin 2 promotes endoplasmic reticulum stress. J Biol Chem. 2012; 287:20321–20332. [PubMed: 22511781]

Novak A, Guo C, Yang W, Nagy A, Lobe CG. Z/EG, a double reporter mouse line that expresses enhanced green fluorescent protein upon Cre-mediated excision. Genesis. 2000; 28:147–155. [PubMed: 11105057]

Ozcan L, Ergin AS, Lu A, Chung J, Sarkar S, Nie D, Myers MG Jr, Ozcan U. Endoplasmic reticulum stress plays a central role in development of leptin resistance. Cell Metab. 2009; 9:35–51. [PubMed: 19117545]

Papanicolaou KN, Khairallah RJ, Ngoh GA, Chikando A, Luptak I, O'Shea KM, Riley DD, Lugus JJ, Colucci WS, Lederer WJ, et al. Mitofusin-2 maintains mitochondrial structure and contributes to stress-induced permeability transition in cardiac myocytes. Mol Cell Biol. 2011; 31:1309–1328. [PubMed: 21245373]

Papanicolaou KN, Ngoh GA, Dabkowski ER, O'Connell KA, Ribeiro RF Jr, Stanley WC, Walsh K. Cardiomyocyte deletion of mitofusin-1 leads to mitochondrial fragmentation and improves tolerance to ROS-induced mitochondrial dysfunction and cell death. Am J Physiol Heart Circ Physiol. 2012; 302:H167–179. [PubMed: 22037195]

Pham AH, Meng S, Chu QN, Chan DC. Loss of Mfn2 results in progressive, retrograde degeneration of dopaminergic neurons in the nigrostriatal circuit. Hum Mol Genet. 2012; 21:4817–4826. [PubMed: 22859504]

Rowland AA, Voeltz GK. Endoplasmic reticulum-mitochondria contacts: function of the junction. Nat Rev Mol Cell Biol. 2012; 13:607–625. [PubMed: 22992592]

Sebastian D, Hernandez-Alvarez MI, Segales J, Sorianello E, Munoz JP, Sala D, Waget A, Liesa M, Paz JC, Gopalacharyulu P, et al. Mitofusin 2 (Mfn2) links mitochondrial and endoplasmic reticulum function with insulin signaling and is essential for normal glucose homeostasis. Proc Natl Acad Sci U S A. 2012; 109:5523–5528. [PubMed: 22427360]

Sisley S, Sandoval D. Hypothalamic control of energy and glucose metabolism. Rev Endocr Metab Disord. 2011; 12:219–233. [PubMed: 21695389]

Wallingford N, Perroud B, Gao Q, Coppola A, Gyengesi E, Liu ZW, Gao XB, Diament A, Haus KA, Shariat-Madar Z, et al. Prolylcarboxypeptidase regulates food intake by inactivating alpha-MSH in rodents. J Clin Invest. 2009; 119:2291–2303. [PubMed: 19620781]

Wardlaw SL. Hypothalamic proopiomelanocortin processing and the regulation of energy balance. European journal of pharmacology. 2011; 660:213–219. [PubMed: 21208604]

Williams KW, Elmquist JK. From neuroanatomy to behavior: central integration of peripheral signals regulating feeding behavior. Nat Neurosci. 2012; 15:1350–1355. [PubMed: 23007190]

Won JC, Jang PG, Namkoong C, Koh EH, Kim SK, Park JY, Lee KU, Kim MS. Central administration of an endoplasmic reticulum stress inducer inhibits the anorexigenic effects of leptin and insulin. Obesity (Silver Spring). 2009; 17:1861–1865. [PubMed: 19543218]

Xu AW, Kaelin CB, Takeda K, Akira S, Schwartz MW, Barsh GS. PI3K integrates the action of insulin and leptin on hypothalamic neurons. J Clin Invest. 2005; 115:951–958. [PubMed: 15761497]

Youle RJ, van der Bliek AM. Mitochondrial fission, fusion, and stress. Science. 2012; 337:1062–1065. [PubMed: 22936770]

Zhang X, Zhang G, Zhang H, Karin M, Bai H, Cai D. Hypothalamic IKKbeta/NF-kappaB and ER stress link overnutrition to energy imbalance and obesity. Cell. 2008; 135:61–73. [PubMed: 18854155]

Zorzano A, Liesa M, Sebastian D, Segales J, Palacin M. Mitochondrial fusion proteins: dual regulators of morphology and metabolism. Seminars in cell & developmental biology. 2010; 21:566–574. [PubMed: 20079867]

HIGHLIGHTS

- POMC neuron mitochondrial dynamics and ER interactions are altered in DIO mice.
- Mfn2-deleted POMC neuron mice are obese due to ER stress-induced leptin resistance.
- Mfn2 deficiency in POMC neurons leads to reduced α-MSH production.
- Central relieve of ER stress rescues the phenotype caused by Mfn2 deletion.

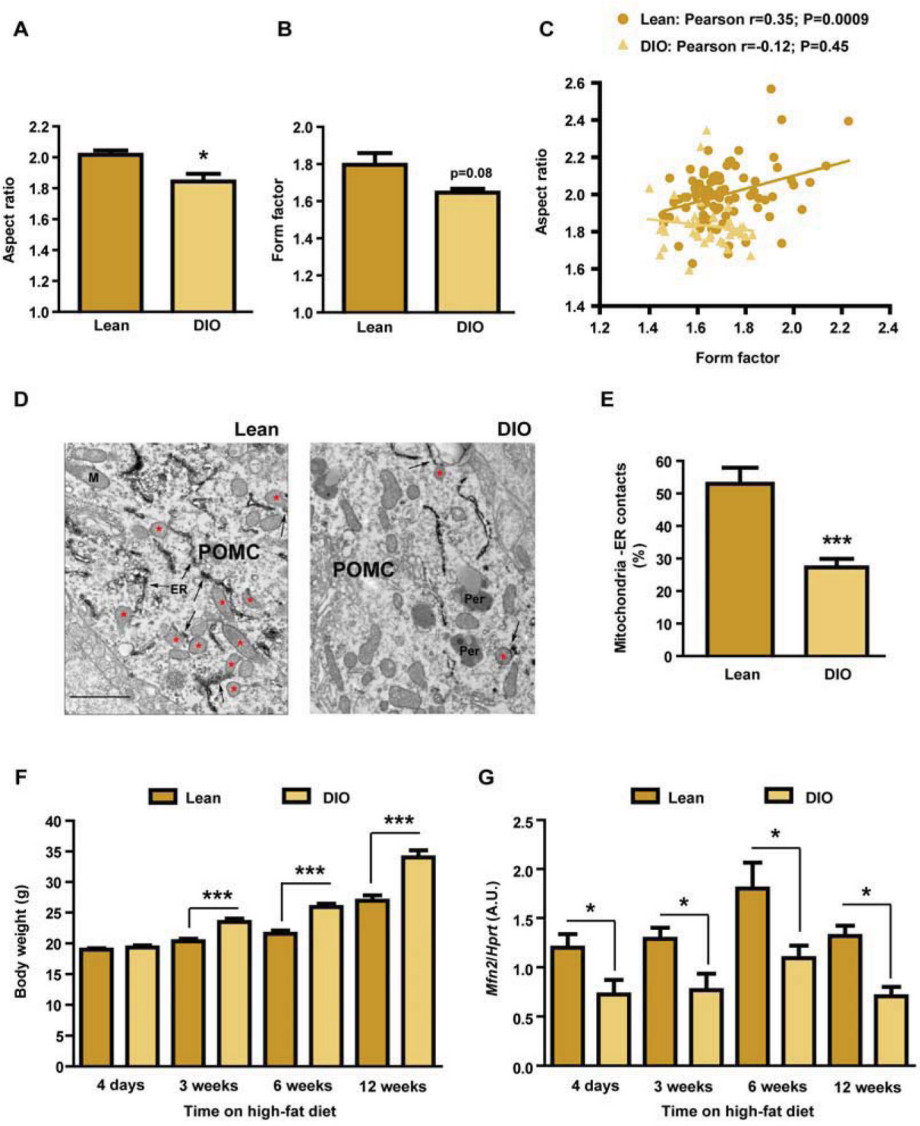

Figure 1. Mitochondrial network complexity and mitochondria-ER contacts in POMC neurons are altered in DIO mice

(A–C) Mitochondrial network complexity analysis in POMC neurons from 18-week old male C57Bl/6 lean and DIO mice.

(D) Representative electron microscopy images and (E) quantification of mitochondria-ER contacts in POMC neurons from male C57Bl/6 lean and DIO mice. Red asterisks show mitochondria in contact with ER (arrows). Note reduced number of mitochondria-ER contacts in POMC neurons from DIO mice. ER: endoplasmic reticulum; Per: peroxisome.

(F) Body weight and (G) *Mfn2* expression levels in the hypothalamus of lean and DIO mice at different time points during a high-fat diet time-course study (n=7–8/group/time point). Data are expressed as mean ± SEM. **P*<0.05. ****P*<0.001. See also Figure S1.

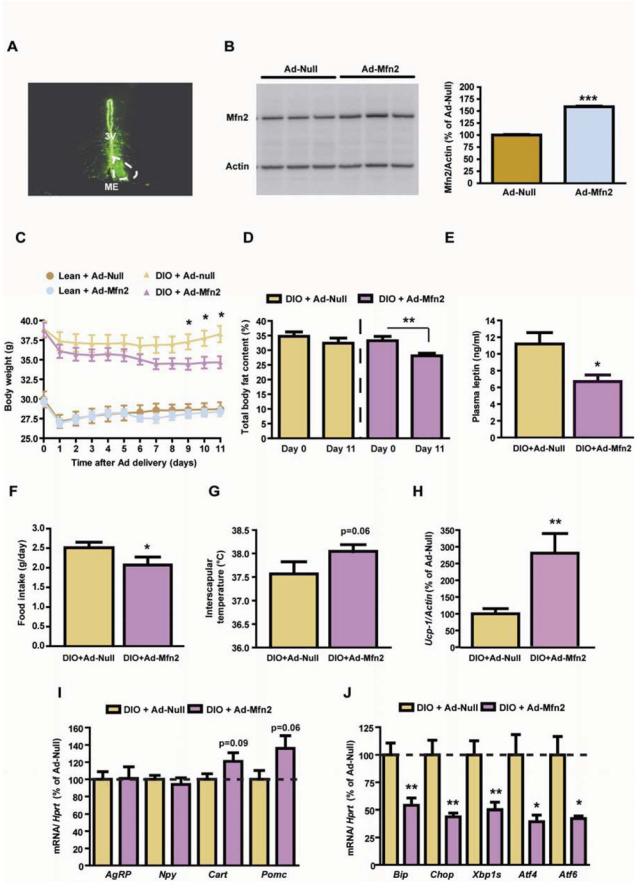

Figure 2. Adenoviral-mediated overexpression of Mfn2 in the ARC of DIO mice ameliorates their metabolic disturbances

(A) Localization studies using an Ad-GFP showing specific delivery in the mouse ARC. For comparative purposes infection in one side of the ARC is shown. 3V: third ventricle; ME: median eminence.

(B) Mfn2 western blot and densitometric quantification of ARC-enriched lysates 3 days after the delivery of Ad-Null or Ad-Mfn2. Loading control (β-Actin) is shown.

(C) Body weight profile, (D) adiposity, (E) plasma leptin, (F) food intake and (G) interscapular temperature.

(H) Expression of thermogenic marker *Ucp-1* in BAT. Probe for *Actin* was used to adjust for total RNA content.

(I) Hypothalamic expression of neuropeptides and (J) ER stress markers. Probe for *Hprt* was used to adjust for total RNA content.

All studies were conducted in male 18 week old lean and/or DIO mice injected intra-ARC with Ad-Null or Ad-Mfn2 (n=10/group). Data are expressed as mean ± SEM. **P*<0.05; ***P*<0.01.

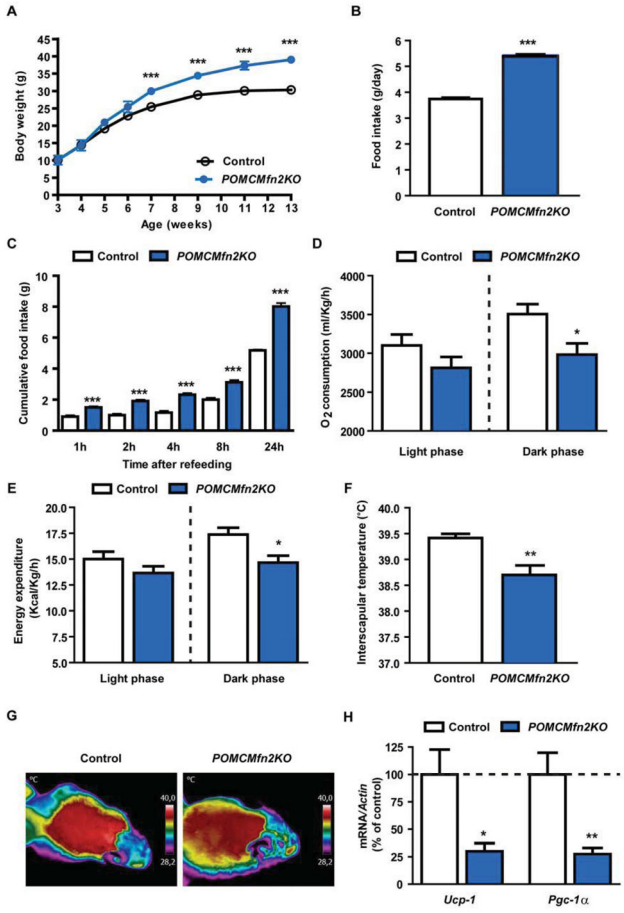

Figure 3. Mice lacking Mfn2 in POMC neurons are obese due to increased food intake and reduced thermogenesis

(A) Body weight profile on chow diet.

(B) Daily food intake in control (n=6) and *POMCMfn2KO* (n=13) mice.

(C) Fast-refeeding test in control (n=6) and *POMCMfn2KO* (n=13) mice.

(D) Daily oxygen consumption and (E) energy expenditure in control (n=7) and *POMCMfn2KO* (n=8) mice.

(F) Basal interscapular temperature adjacent to the BAT depot and (G) representative thermographic images of control (n=6) and *POMCMfn2KO* (n=7) mice.

(H) Gene expression analysis of thermogenic markers in BAT from control (n=6) and *POMCMfn2KO* (n=6) mice. Probe for *Actin* was used to adjust for total RNA content.

All studies were conducted in male 12–14 week old control and *POMCMfn2KO* mice. Data are expressed as mean ± SEM. **P*<0.05; ***P*<0.01; ****P*<0.001. See also Figure S2.

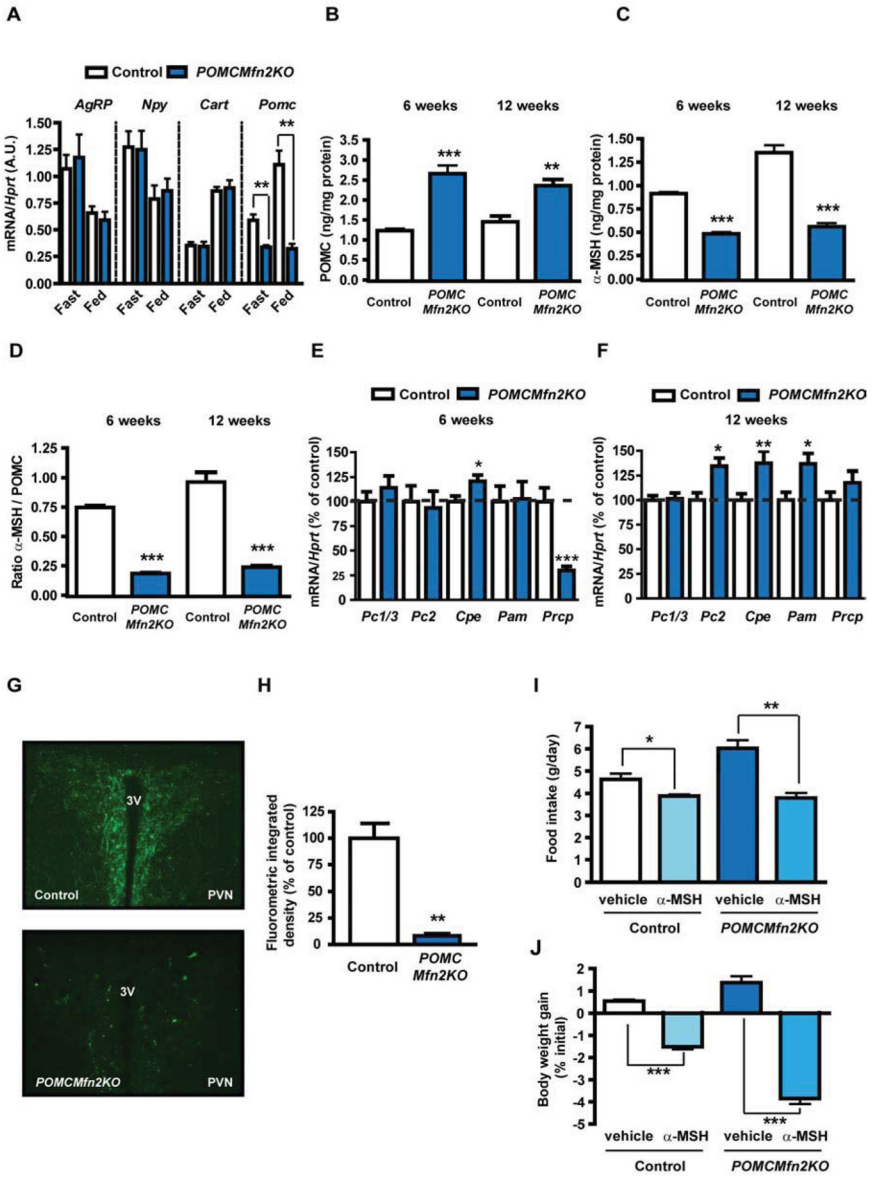

Figure 4. Loss of Mfn2 in POMC neurons causes defective POMC processing

(A) Neuropeptide expression in the hypothalamus from 12-week old male control (n=6–10) and *POMCMfn2KO* (n=6) mice under fed and fasting conditions. Probe for *Hprt* was used to adjust for total RNA content.

(B) Total hypothalamic POMC and (C) α-MSH content in 6 and 12-week old male control (n=6) and *POMCMfn2KO* (n=7) mice.

(D) POMC processing as measured by α-MSH/POMC ratio.

(E–F) Expression analysis of POMC processing genes in the hypothalamus from 6 and 12-week old male control (n=9–13) and *POMCMfn2KO* (n=6–8) mice.

(G) Representative immunofluorescence images showing α-MSH staining in the PVN from 12-week old male control (n=3) and *POMCMfn2KO* (n=3) mice and (H) integrated density quantification.

(I) Food intake and (J) body weight gain in 12-week old male control (n=4) and *POMCMfn2KO* (n=5) mice after acute i.c.v. injection of α-MSH.

Data are expressed as mean ± SEM. *P<0.05; **P<0.01; ***P<0.001. 3V: third ventricle. PVN: paraventricular nucleus. See also Figure S3.

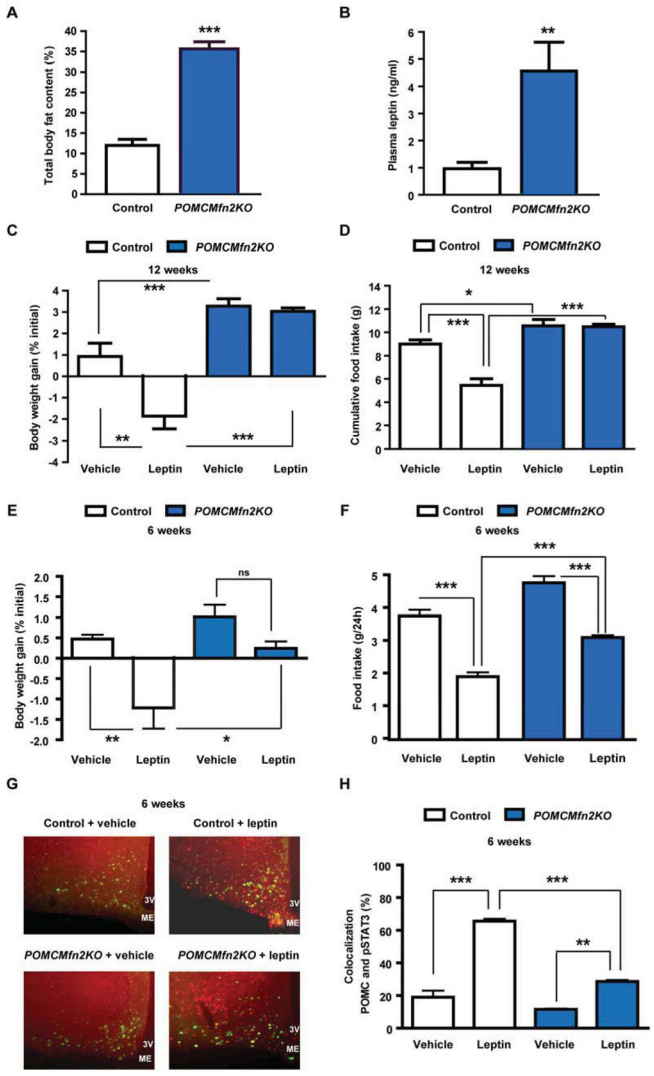

Figure 5. Deficiency of Mfn2 in POMC neurons leads to primary leptin resistance

(A) Body fat content and (B) plasma leptin in male control (n=6) and *POMCMfn2KO* (n=7) mice at 12–14 weeks of age.

(C–D) Body weight gain and cumulative food intake in 12–14 week old male control (n=7) and *POMCMfn2KO* (n=8) mice after 3-day leptin injection.

(E–F) Daily body weight gain and food intake in 6-week old male control (n=6) and *POMCMfn2KO* (n=6) mice after an acute leptin sensitivity test.

(G–H) Representative images showing double immunofluorescence examining pStat3 in POMC neurons and percentage of colocalization after vehicle or leptin stimulation in 6 week old POMCZ/EG (n=3) and *POMCMfn2KOZEG* (n=3) mice.

Data are expressed as mean ± SEM. **P*<0.05; ***P*<0.01; ****P*<0.001. 3V: third ventricle. ME: median eminence. ns: not significant. See also Figures S4.

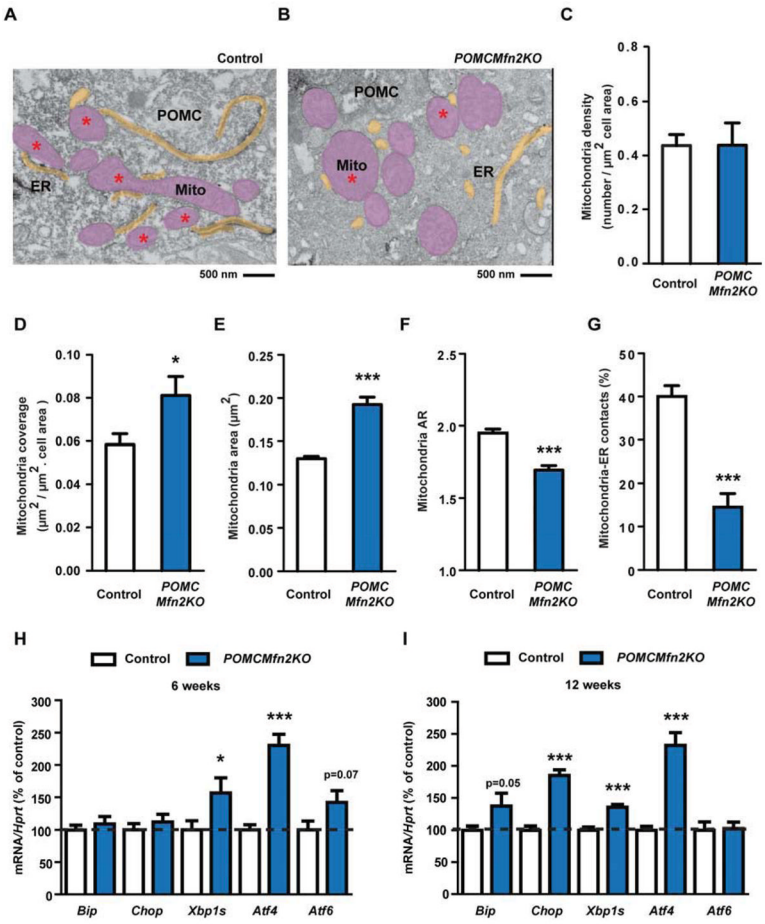

Figure 6. Deletion of Mfn2 in POMC neurons alters mitochondrial morphology, mitochondrial-ER contacts and induces ER stress

(A–B) Representative electron microscopy images of POMC neurons from 12-week old male control (A) and *POMCMfn2KO* (B) mice. Mitochondria (Mito: pink areas) and endoplasmic reticulum (ER: yellow areas) are shown. Red asterisk shows mitochondria in contact with ER.

(C) Mitochondria density, (D) mitochondria coverage, (E) mitochondria area and (F) mitochondria aspect ratio (AR) in POMC neurons from 12-week old male control (n=5; 1198 mitochondria from 30 POMC neurons) and *POMCMfn2KO* (n=3; 530 mitochondria from 15 POMC neurons) mice.

(G) Percentage of mitochondria-ER contacts in POMC neurons from 12-week old male control (n=5; 32 POMC neurons) and *POMCMfn2KO* (n=3; 17 POMC neurons) mice.

(H) Gene expression analysis of ER-stress markers in the hypothalamus from 6-week old male control (n=10–15) and *POMCMfn2KO* (n=8–12) mice.

(I) Gene expression analysis of ER-stress markers in the hypothalamus from 12-week old male control (n=21–23) and *POMCMfn2KO* (n=16–18) mice. Probe for *Hprt* was used to adjust for total RNA content.

Data are expressed as mean ± SEM. **P*<0.05; ****P*<0.001. See also Figures S5.

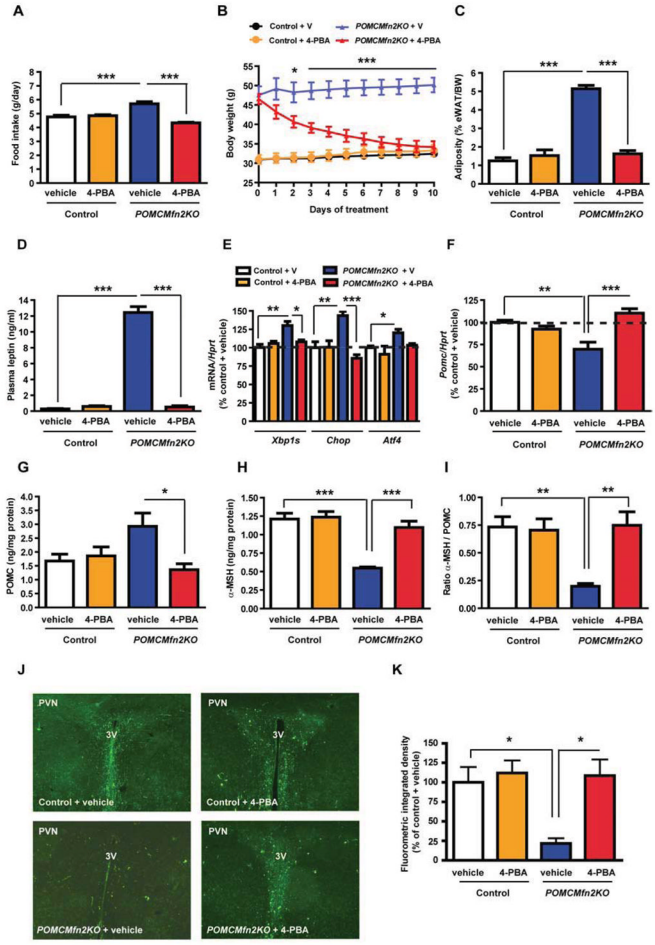

Figure 7. Restoration of energy homeostasis in *POMCMFN2KO* mice by 4-phenyl butyric acid (4-PBA) administration

Effects of 10-day i.c.v. 4-PBA administration in 14-week old male control (n=8) and *POMCMfn2KO* (n=8) mice on:

(A) Daily food intake.

(B) Body weight.

(C) Adiposity.

(D) Plasma leptin.

(E) Expression of ER stress markers in the hypothalamus (n=4/genotype/treatment).

(F) *Pomc* mRNA expression (n=4/genotype/treatment).

(G) Hypothalamic POMC content (n=4/genotype/treatment).

(H) Hypothalamic α-MSH content (n=4/genotype/treatment).

(I) α-MSH/POMC ratio.

(J) Representative immunofluorescence images showing α-MSH staining in the PVN and (K) integrated density quantification (n=3/genotype/treatment).

Probe for *Hprt* was used to adjust for total RNA content. Data are expressed as mean ± SEM. **P*<0.05; ***P*<0.01; ****P*<0.001. eWAT: epididymal white adipose tissue; BW: body weight; V: vehicle. 3V: third ventricle. PVN: paraventricular nucleus. See also Figure S6.